## Reviewer

**I have now received to reviews for your manuscript entitled "Variation of sediment supply by periglacial debris flows at Zelunglung in the eastern syntaxis of Himalayas since the 1950 Assam Earthquake". Both reviewers highlight the high quality of your work, in particular noting the integration of diverse data. While the second referee requests only a few techical corrections, the first reviewer has a few suggestions for further improving your work in particular concerning the quantification of uncertainties. Also, the reviewer notes that there should be a better separation of the results and discussion chapter.**

**To go forward with your manuscript, please address the points raised by the reviewers. I am looking forward to your revisions in due time.**

Thank you for your constructive suggestions. In response to your comments regarding the quantification of uncertainties and the structure of the manuscript (results and discussion chapter), we have made targeted revisions, which are detailed in the following point-by-point responses:

### 1. Quantification of Uncertainties

- **Author's response：**

Thank you for your constructive suggestions. We have made the following targeted revisions:

1) In Section 3.2.2 “Drone image interpretation,” we clarified the quantification methods for DoD uncertainty and volume estimation uncertainty.
2) In Section 4.2 “Sediment characteristics of the 2020 event,” we provided the arithmetic mean, RMSE, maximum, minimum, and standard deviation of the DoD values in the stable areas, and quantified the uncertainty of the volume estimation using the two-sigma DoD uncertainty. In addition, we updated Figure 9 (formerly Figure 10) to display the DoD values of the stable areas.
3) In Section 5.5 “Uncertainties,” we discussed the sources of errors in DoD and volume estimation, as well as the uncertainties associated with NVA interpretation.

- **Author's changes in manuscript:**

We have revised or added descriptions in the following sections:

3.2.2 Drone image interpretation

To determine the uncertainty in our DoD differencing result we followed methods outlined in Shugar et al. (2021). Fifteen stable areas on old debris flow terraces adjacent to the valley floor, mainly roads and unseeded farmlands, were identified. The standard deviation of DoD values within these areas was calculated and used to estimate a two-sigma DoD uncertainty. We assumed that the errors of all DoD grid cells have the same direction, providing a conservative estimate of the total sediment volume evacuated from the catchment (Anderson, 2019).

## 4.2 Sediment characteristics of the 2020 event

Comparing the DSMs before and after the 2020 event, the maximum erosional depth reached 20.47 m, with a mean depth of 4.17 m in the downstream channel. The maximum deposition depth was 13.51 m, and the mean depth was 3.4 m in the depositional fan (Fig. 9b). The mean DoD value across the 15 stable areas was −0.032 m, with an RMSE of 0.24 m, a maximum of 0.295 m, a minimum of −0.383 m, and a standard deviation of 0.247 m. Accordingly, the two-sigma DoD uncertainty was 0.493 m (Figs. 9a-b). Based on the DoD, we estimated that a total of $12.8\times10^4$ $m^3$ (two-sigma confidence intervals $10.95\times10^4$-$14.66\times10^4$ $m^3$) of debris was transported out of the catchment (Fig. 9b).

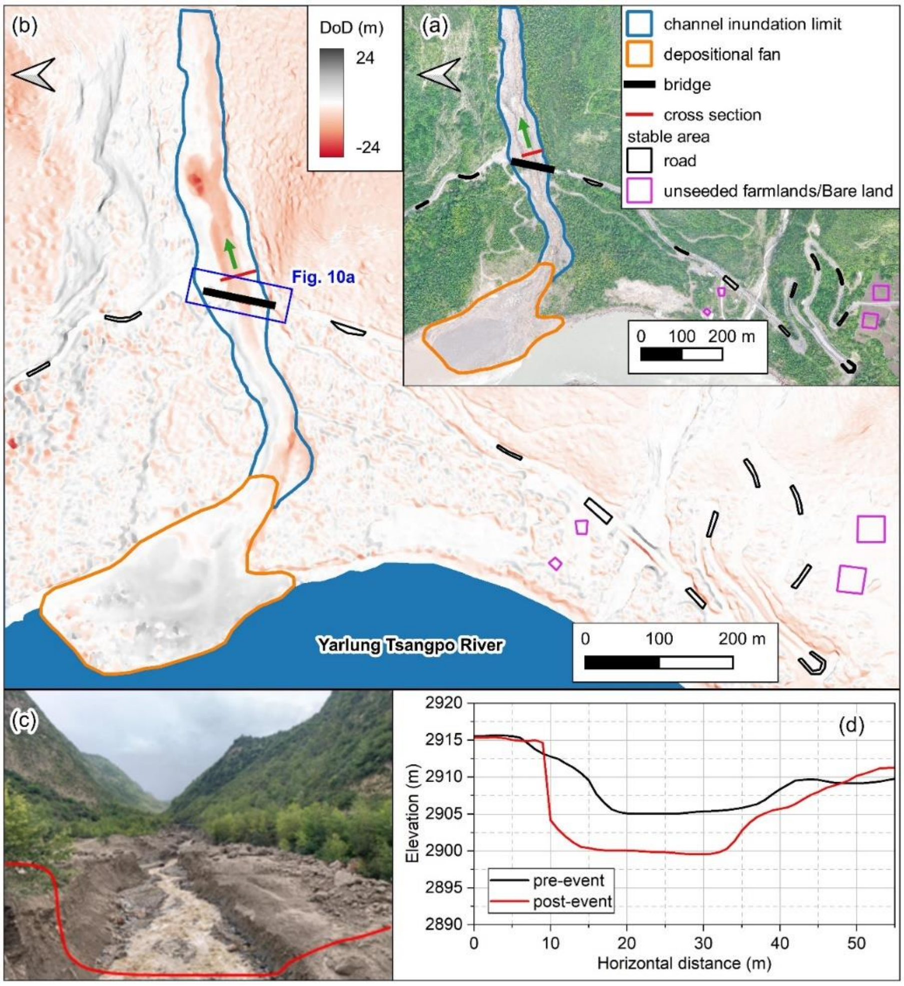


**Figure 9: Geomorphic changes of the downstream channel and alluvial fan after the debris flows of 2020. (a) Post-event UAV digital orthophoto map of the ZLL downstream area and its surrounding area. (b) Erosion and deposit depth caused by the debris flows. (c) Photo of the channel after the debris flows (photo taken on 11 Sep 2020). The red line represents the cross-**

**section next to the Zhibai Bridge, and the camera angle direction is denoted by green arrow in figure a-b. (d) Cross-sections before (black) and after (red) the debris flows.**

## 5.5 Uncertainties

The uncertainty of the DoD arises from multiple sources. On the one hand, the positional accuracy of the onboard GPS used to produce the UAV-derived DSMs is limited (Niu et al., 2024). On the other hand, surface characteristics such as vegetation and canopy cover, as well as flight parameters and environmental factors (e.g., illumination, shadow, and surface moisture), can also affect the quality of DSM reconstruction(Anders et al., 2020; Chaudhry et al., 2021; Kucharczyk et al., 2018). To minimize these uncertainties, several geomorphically stable ground control points (GCPs) were manually selected and used for co-registration between the two DSMs. Nevertheless, potential errors associated with GCP positioning, number, and spatial distribution cannot be entirely excluded (Han et al., 2019). Despite these limitations, our two-sigma DoD uncertainty (±0.493 m) falls within the reasonable range reported in previous studies (Müller et al., 2014; Prokešová et al., 2010). It should also be noted that, although the most recent pre- and post-event DSMs were used to reconstruct the debris-flow evacuation volume, our results may underestimate the actual evacuated material, as the UAV data were acquired during a period of high discharge in the main river, when some of the mobilized sediments might have been transported away or submerged.

Previous studies have shown that debris-flow volume is often empirically related to the extent of the inundation area (e.g., Iverson et al., 1998), which supports the use of NVA as a proxy for sediment volume. The absence of systematic depositional thickness measurements prevents direct conversion of NVAs into absolute debris-flow volumes, so NVA only reflects relative fluctuations rather than precise values. Moreover, the empirical relationship between inundation area and debris-flow volume may vary with local geomorphic and hydrological conditions, such as fan slope and gully confinement, further complicating volume inference and limiting the applicability of uniform statistical error models. In practice, the NVA includes a fixed portion of the area inundated by the main river and is therefore slightly larger than the actual depositional area caused by debris flows. Technically, the contribution of the main river to NVA cannot be entirely excluded. Nevertheless, the riverbank line remained stable from the 1980s to the 2010s, during which no large periglacial debris flows occurred (Figs. 11b and c; Zhang and Shen, 2011), and the remote-sensing images we used were taken in similar seasons. It is therefore reasonable to assume that variations in river water level have little influence on changes in NVA. The one-grid cell uncertainty in the interpretation of the NVA ultimately translates into uncertainty in its representation of sediment volume (Fig. 11e). The magnitude of this uncertainty depends on factors such as the co-registration accuracy between the secondary and primary images, the time interval between image acquisitions, surface conditions (e.g., shadows), and the spatial resolution of the imagery (Paul et al., 2022). Although these uncertainties cannot be completely eliminated, their influence on the overall trend of NVA variation is minor and thus does not alter the main analytical results and conclusions.

While accurate estimation of sediment volume from NVA is beyond the scope of this study, we acknowledge the associated uncertainties, which warrant more rigorous treatment in future study. Future studies that integrate high-resolution LiDAR, UAV photogrammetry, or borehole surveys with field-based volume measurements could provide more robust statistical assessments of the NVA–volume relationship. The application of dense stereo-pair techniques for DSM extraction from historical and modern satellite archives also has considerable potential to provide three-dimensional constraints on sediment thickness and deposition, thereby improving the translation from inundation area to sediment volume.

2. **The reviewer notes that there should be a better separation of the results and discussion chapter.**

- **Author's response：**

Thank you for your constructive comments. We have moved the extended discussion that was previously included in the Results chapter to a newly added Section 5.1, "Erosion and sedimentation of periglacial debris flows," in the Discussion chapter. The revised Results chapter now objectively presents the characteristics of historical debris-flow events (based on literature review), the features of the 2020 event, and the NVA changes on the depositional fan, focusing on the "data, imagery, and trends" directly derived from the applied methodologies. The newly added Section 5.1 mainly discusses the depositional characteristics and mechanisms of glacial debris flows based on the sedimentary phenomena observed during the 2020 event.

Due to these structural changes, some figures have been updated, and their order within the manuscript has also been adjusted.

- **Author's changes in manuscript:**

Due to the structural adjustments, presenting all the changes here would be redundant. Since the Results chapter was only streamlined and its logical order reorganized, we focus here on presenting the newly added discussion content here. For detailed revisions to the Results chapter, please refer to the manuscript.

5.1 Erosion and sedimentation of periglacial debris flows

The 2020 event was characterized by strong entrainment capacity and a pronounced volume growth effect. The initiation area of the 2020 event was often covered by snow and ice, and the ice-snow melting water easily infiltrates into the debris-ice mixtures. Once the slope material was entrained into the mass flow, such a nearly saturated mixture could quickly turn into a debris flow.

Peng et al. (2022) estimated a debris loss of 1.14 Mm3 in the scarp area except for the initiated ice and rock. But they mistake the hillslope below the cliff as the source area of the event. That means the volume of the debris mass flowed downward into the south channel should include half of the initiated ice-rock mass and the debris loss of 1.14 $Mm^3$. The entrained volume is at least 16 times the initiated volume. In addition, eyewitnesses observed two surges in the outlet, one of which may have resulted from two ice-rock avalanches with different volumes probably happened on the ridge. But it is more likely that there was only one ice-rock avalanche during the event, but a synchronization of the ice-rock impacts in the scarp area. The blockage by large boulders and the induced landslides on the narrow channel resulted in two successive debris-flow surges, which ultimately amplified the magnitude of the debris flows (Fig. 6d) (Cui et al., 2013; Li et al., 2025; Liu et al., 2020).

The field evidence shows some features of periglacial debris-flow transportation that differ from fluvial transport. Periglacial debris flows can transport rocks or boulders not only in midstream steep channels but also in gentle downstream channels or alluvial fans. In the downstream channel, with an average gradient of 13.8%, a relatively high velocity (~10 m/s) enabled the flows to mobilize boulders of 5.0 meters in diameter (Costa, 1983). The transportation mode of coarse grains is a kind of “Relay-race style”, one event by one event. The angularity of the fragmented rocks in the upstream reduced their mobility, and the attenuated overland flow had less transport capacity, causing most of the angular rocks resided in the upslope or upstream channel and did not move downward. The large sub-rounded or sub-angular boulders in the lower reaches came from the middle of the downstream reaches. We guess that grain segregation happened initially, and only fine parts of the ice-rock mass and melting water traveled downward the midstream. The resident angular rocks would be rounded gradually by the periglacial stream and transported downward by the subsequent floods or debris flows.

In the downstream reach, slope and flow depth are critical factors controlling the boulder transport. Interstitial slurry among the boulders could separate from the boulders when the debris flows moved on a gentle slope or spread over an open fan (Fig. 7c). The interstitial slurry provided buoyancy for the boulders and reduced resistance between them and the bed. Once there was no interstitial slurry, the boulders stopped quickly. The large stones easily slowed down when the flow depth and the velocity decreased on the edges of the debris flows. When the debris flows moved to A1, the flow depth was far higher than the channel depth. Many coarse particles were left on the highland. When the debris flow enters the bend at a high speed, a large velocity difference will be generated on the concave-convex bank, i.e., the super-elevation effect (Chen et al., 2009). The debris flows produced the super-elevation effect when they moved to A2, a partially curved channel. Then, some coarse particles overflowed the channel and deposited on the A2 banks. When the debris flows moved out the catchment outlet and had no boundary constraint, the other coarse particles gradually deposited from the fan top to the fan edge due to loss of kinetic energy (Fig. 8a). The distinct depositional units in A1 and A3 reflect the gradual accumulation of multiple debris-flow surges (Sohn, 2000; Major, 1998), which may correspond to the two successive debris-flow surges in ZLL at 5:00 pm and 6:00 pm.

Debris flows usually have steep coarse-grained surge fronts (snouts) and inter-surge watery flows (McCoy et al., 2013; Yan et al., 2023). The periglacial debris flows in ZLL had similar spatial compositions. The granular flows (coarse-grained snouts) at the fronts exerted a powerful impact on obstacles, and the inter-surge watery flows or water-rich tails with relatively low sediment concentration played critical roles in erosion. Peng et al. (2022) numerically simulated the final erosion and deposition along the flow path. The maximum erosion depth was 7.41 m at the beginning of the downstream channel. We think the simulation underestimates the erosion depth because the final erosion accumulates several erosive watery flows. It is noteworthy that, as the DSM data were acquired during the high-flow season of the Yarlung Tsangpo River, part of the deposited material may have been eroded or submerged by the river, leading to an underestimation of the actual volume of sediment transported out of the catchment.

### 3. Other changes by the author

We have further polished the English wording.

Reference:


Anders, N., Smith, M., Suomalainen, J., Cammeraat, E., Valente, J., and Keesstra, S.: Impact of flight altitude and cover orientation on Digital Surface Model (DSM) accuracy for flood damage assessment in Murcia (Spain) using a fixed-wing UAV, EARTH SCI INFORM, 13, 391–404, https://doi.org/10.1007/s12145-019-00427-7, 2020.

Anderson, S. W.: Uncertainty in quantitative analyses of topographic change: error propagation and the role of thresholding, EARTH SURF PROC LAND, 44, 1015–1033, https://doi.org/10.1002/esp.4551, 2019.

Chaudhry, M. H., Ahmad, A., Gulzar, Q., Farid, M. S., Shahabi, H., and Al-Ansari, N.: Assessment of DSM Based on Radiometric Transformation of UAV Data, SENSORS-BASEL, 21, 1649, https://doi.org/10.3390/s21051649, 2021.

Chen, N., Yang, C., Li, Z., and He, J.: Research on the Relationship between the Calculation of Debris flow Velocity and Its Super Elevation in Bend, Advanced Engineering Sciences, 41, 165–171, https://doi.org/1009-3087(2009)03-0165-07, 2009.

Costa, J. E.: Paleohydraulic reconstruction of flash-flood peaks from boulder deposits in the Colorado Front Range, GEOL SOC AM BULL, 94, 986, https://doi.org/10.1130/0016-7606(1983)94<986:PROFPF>2.0.CO;2, 1983.

Cui, P., Zhou, G. G. D., Zhu, X. H., and Zhang, J. Q.: Scale amplification of natural debris flows caused by cascading landslide dam failures, GEOMORPHOLOGY, 182, 173–189, https://doi.org/10.1016/j.geomorph.2012.11.009, 2013.

Han, Y., Choi, J., Jung, J., Chang, A., Oh, S., and Yeom, J.: Automated Coregistration of Multisensor Orthophotos Generated from Unmanned Aerial Vehicle Platforms, J SENSORS, 2019, 1–10, https://doi.org/10.1155/2019/2962734, 2019.

Iverson, R. M., Schilling, S. P., and Vallance, J. W.: Objective delineation of lahar-inundation hazard zones, GEOL SOC AM BULL, 110, 972–984, https://doi.org/10.1130/0016-7606(1998)110<0972:ODOLIH>2.3.CO;2, 1998.

Kucharczyk, M., Hugenholtz, C. H., and Zou, X.: UAV–LiDAR accuracy in vegetated terrain, J UNMANNED VEH SYST, 6, 212–234, https://doi.org/10.1139/juvs-2017-0030, 2018.

Li, H., Hu, K., Liu, S., Cheng, H., Wen, Z., Zhang, X., Ma, C., Gouli, M. R., Wei, L., and Yang, H.: Abundant antecedent rainfall incubated a group-occurring debris flow event in the Dadu River Basin, Southwest China, LANDSLIDES, 22, 1955–1971, https://doi.org/10.1007/s10346-025-02489-9, 2025.

Liu, M., Zhang, Y., Tian, S., Chen, N., Mahfuzr, R., and Javed, I.: Effects of loose deposits on debris flow processes in the Aizi Valley, southwest China, J MT SCI-ENGL, 17, 156–172, https://doi.org/10.1007/s11629-019-5388-9, 2020.

Major, J. J.: Pebble orientation on large, experimental debris-flow deposits, SEDIMENT GEOL, 117, 151–164, https://doi.org/10.1016/S0037-0738(98)00014-1, 1998.

McCoy, S. W., Tucker, G. E., Kean, J. W., and Coe, J. A.: Field measurement of basal forces generated by erosive debris flows, J GEOPHYS RES-EARTH, 118, 589–602, https://doi.org/10.1002/jgrf.20041, 2013.

Müller, J., Gärtner-Roer, I., Thee, P., and Ginzler, C.: Accuracy assessment of airborne photogrammetrically derived high-resolution digital elevation models in a high mountain environment, ISPRS J PHOTOGRAMM, 98, 58–69, https://doi.org/10.1016/j.isprsjprs.2014.09.015, 2014.

Niu, Z., Xia, H., Tao, P., and Ke, T.: Accuracy Assessment of UAV Photogrammetry System with RTK Measurements for Direct Georeferencing, ISPRS Ann. Photogramm. Remote Sens. Spatial Inf. Sci., X-1–2024, 169–176, https://doi.org/10.5194/isprs-annals-X-1-2024-169-2024, 2024.

Paul, F., Piermattei, L., Treichler, D., Gilbert, L., Girod, L., Kääb, A., Libert, L., Nagler, T., Strozzi, T., and Wuite, J.: Three different glacier surges at a spot: what satellites observe and what not, CRYOSPHERE, 16, 2505–2526, https://doi.org/10.5194/tc-16-2505-2022, 2022.

Peng, D., Zhang, L., Jiang, R., Zhang, S., Shen, P., Lu, W., and He, X.: Initiation mechanisms and dynamics of a debris flow originated from debris-ice mixture slope failure in southeast Tibet, China, Engineering Geology, 307, 106783, https://doi.org/10.1016/j.enggeo.2022.106783, 2022.

Prokešová, R., Kardoš, M., and Medveďová, A.: Landslide dynamics from high-resolution aerial photographs: A case study from the Western Carpathians, Slovakia, GEOMORPHOLOGY, 115, 90–101, https://doi.org/10.1016/j.geomorph.2009.09.033, 2010.

Shugar, D. H., Jacquemart, M., Shean, D., Bhushan, S., Upadhyay, K., Sattar, A., Schwanghart, W., McBride, S., de Vries, M. V. W., Mergili, M., Emmer, A., Deschamps-Berger, C., McDonnell, M., Bhambri, R., Allen, S., Berthier, E., Carrivick, J. L., Clague, J. J., Dokukin, M., Dunning, S. A., Frey, H., Gascoin, S., Haritashya, U. K., Huggel, C., Kääb, A., Kargel, J. S., Kavanaugh, J. L., Lacroix, P., Petley, D., Rupper, S., Azam, M. F., Cook, S. J., Dimri, A. P., Eriksson, M., Farinotti, D., Fiddes, J., Gnyawali, K. R., Harrison, S., Jha, M., Koppes, M., Kumar, A., Leinss, S., Majeed, U., Mal, S., Muhuri, A., Noetzli, J., Paul, F., Rashid, I., Sain, K., Steiner, J., Ugalde, F., Watson, C. S., and Westoby, M. J.: A massive rock and ice avalanche caused the 2021 disaster at Chamoli, Indian Himalaya, Science, 373, 300–306, https://doi.org/10.1126/science.abh4455, 2021.

Sohn, Y. K.: Coarse-grained debris-flow deposits in the Miocene fan deltas, SE Korea: a scaling analysis, SEDIMENT GEOL, 130, 45–64, https://doi.org/10.1016/S0037-0738(99)00099-8, 2000.

Yan, Y., Tang, H., Hu, K., Turowski, J. M., and Wei, F.: Deriving Debris-Flow Dynamics From Real-Time Impact-Force Measurements, J GEOPHYS RES-EARTH, 128, e2022JF006715, https://doi.org/10.1029/2022JF006715, 2023.

Zhang, J. and Shen, X.: Debris-flow of Zelongnong Ravine in Tibet, J. Mt. Sci., 8, 535–543, https://doi.org/10.1007/s11629-011-2137-0, 2011.